Feature Enhancement and Extraction Method of Parallel Arc Fault in Three-Phase Motor and Frequency Converter Load Circuit

Hongxin Gao, *Member, IEEE*, Yuze Lv, Zhiyong Wang, *Member, IEEE*, and Jiacheng Cai

***Abstract*—The parallel arc fault is one of the most important causes of electrical fire. However, there is no effective detection method for parallel arc fault. To solve this problem, a fault feature enhancement method based on energy transformation and reconstruction of modal components and a fault feature extraction method based on non-negative matrix factorization were proposed. First, the parallel arc fault experiments under different load current and current-limiting resistor conditions were carried out in the three-phase motor and frequency converter load circuit. Second, the current signal was decomposed into k modal components by using adaptive empirical wavelet transform, and the energy transformation and reconstruction of each modal component were performed in turn to enhance the fault features. Third, the parallel arc fault features were extracted from the enhancement signals by using two-stage non-negative matrix factorization dimension reduction. Finally, the performance of the fault feature enhancement and extraction method was tested by using the identification model established with a least squares support vector machine. The results indicated that the proposed method can effectively enhance and extract the parallel arc fault features from the current signals, and the detection accuracy of the parallel arc fault can reach more than 95%.**

***Index Terms*—Fault detection, feature enhancement, feature extraction, parallel arc fault.**

I. Introduction

THREE-PHASE motor and frequency converter are typical industrial loads with a large number of applications. The power supply and distribution lines are often subjected to external forces such as extrusion, impact, and dragging during the operation of mechanical equipment, so as to cause the insulation damage of the lines. In addition, the industrial environment is very bad. Due to the influence of many factors such as line overheating, environment humidity, light irradiation, chemical erosion, and the insulation of the line will be aged. The above factors will most likely cause the insulation performance among the phase lines of the circuit to decrease. It will further cause the insulation to be broken down, so as to lead to a parallel arc fault. The temperature of the parallel arc fault is extremely high, which is much higher than the ignition point of combustible materials such as cable insulation. The parallel arc fault is one of the main causes of electrical fire. Although the parallel arc fault is caused by the short-circuit, the parallel arc fault often occurs in the high-resistance state in the initial stage, which will limit the current amplitude. So, the fault current amplitude is smaller than the short-circuit current of the metallic short-circuit fault [1]. It will affect the correct judgment of the conventional short-circuit protection device, so as to cause safety accidents such as device damage or electrical fire. Therefore, it is of great significance to study a detection method of the parallel arc fault in the industrial three-phase motor and frequency converter load circuit to improve the reliability of industrial power supply and distribution system and avoid the electrical fire.

Due to the current and voltage signals are easy to obtain, the use of features of the current or voltage signal to detect the arc fault is currently a research hotspot. Wu et al. [2] designed a Butterworth bandpass filter with different bandpass frequency for different load types to deal with the current signal, and used the threshold method to detect the series arc fault. Jiang and Zheng [3] adaptively decomposed and reconstructed the coupled high-frequency differential signals according to the spectral features and the desirable margin, and used the Chebyshev distance and the high-order center distance to detect the series arc fault. He et al. [4] extracted the average value of the absolute values, the sum of harmonic amplitudes and wavelet energy entropy of the current signal as the fault features, and used the threshold method to detect the series arc fault. Ding et al. [5] used the absolute difference amplitudes of the neighboring waveforms of the current signal to determine the initial period of the fault, and developed a one-dimensional convolutional neural network (CNN) to identify the random features of the arc fault in the absolute difference to detect the series arc fault. Chen et al. [6] performed all-phase discrete Fourier transform on the current signal, and used a deep learning neural network based on Logistic regression to detect the series arc fault. Ferracuti et al. [7] constructed a gray image by using the current signals, extracted the texture features from the gray co-occurrence matrix images, and used linear discriminant analysis to detect the series arc fault. Wang et al. [8] applied the raw current signal as the input of a

Received 23 October 2024; revised 31 December 2024 and 9 February 2025; accepted 6 March 2025. Date of publication 11 March 2025; date of current version 14 April 2025. This work was supported in part by the National Natural Science Foundation of China under Grant 52077158 and in part by Basic Scientific Research Project of the Education Department of Liaoning Province under Grant LJ212410147022 and Grant LJ242410147030. Recommended for publication by Associate Editor A. M. Trzynadlowski. *(Corresponding author: Hongxin Gao.)*

The authors are with the Faculty of Electrical and Control Engineering, Liaoning Technical University, Huludao 125105, China (e-mail: gaohongxin@lntu.edu.cn).

Color versions of one or more figures in this article are available at https://doi.org/10.1109/TPEL.2025.3549866.

Digital Object Identifier 10.1109/TPEL.2025.3549866

one-dimensional (1-D) CNN, and developed an ArcNet model to detect the series arc fault. Zhang et al. [9] proposed a data expansion method of the series arc fault based on the generative adversarial network, and established an identification model of the series arc fault based on asymmetric CNN. Zhang et al. [10] established a phase space image based on wavelet transform, and developed a ResNet to detect the series arc fault. Zhang et al. [11] extracted the time-frequency features of the current signal by using generalized S-transform, and combined it with a 2-D CNN to detect the series arc fault. Luo et al. [12] reconstructed the current signal by using the wavelet high-frequency detail signals, and extracted the integral, variance, kurtosis and Shannon entropy of the reconstructed signal as the fault features, and developed an XGBoost model to detect the series arc fault. Long et al. [13] calculated the Fourier coefficients, Mel frequency cepstrum coefficients, and wavelet features as the fault features, and developed a multifeature fusion neural network to detect the series arc fault. Zhang et al. [14] selected different spectral feature combinations as the fault features for resistive, inductive, and switchable loads, respectively. And a K-nearest neighbor algorithm was used to detect the series arc fault. Wang et al. [15] decomposed the current signal by using empirical wavelet transform (EWT), calculated the composite entropy of the fifth modal component and the time-domain sensitive features of the current signal as the fault features, and developed a probabilistic neural network to detect the series arc fault. Gao et al. [16] performed a five-layer decomposition on the current signal by using EWT, calculated the singular values of the reconstructed attractor track matrix (RATM) of each decomposed signals as the fault features, and utilized a support vector machine (SVM) to identify the series arc fault. Wang et al. [17] decomposed the current signal by using variational modal decomposition (VMD), calculated the sample entropy and energy entropy as the fault features, and utilized a SVM to identify the series arc fault. Jiang et al. [18] extracted the fault features from the current signals by using an improved complete ensemble empirical mode decomposition (CEEMD) method, reduced the feature dimension by using a TreeBagger function, and applied a random forest to detect the series arc fault. Zhang et al. [19] adopted complete ensemble empirical mode decomposition with adaptive noise (CEEMDAN) and Hilbert transform to extract the fault features from the current signals, and used a long short-term memory (LSTM) network to identify the series arc fault. Zou et al. [20] decomposed the current signal by using CEEMDAN, calculated 16 feature indexes based on time window of the decomposed signals, extracted the fault features by using the maximum mutual information coefficient and the significance of feature changes, and utilized a SVM to identify the series arc fault. Dai et al. [21] extracted the time-domain statistics, frequency-domain indicators, and $L2/L1$ norm of the current signal as the fault features, and used a random forest algorithm to detect the series arc fault. Hwang et al. [22] combined the time-domain statistics with fast Fourier transform based on the phase lock loop information to detect the series arc fault. Cui et al. [23] performed generalized S-transform on the current signal, extracted the root mean square and energy of 2 kHz component as the fault features, and applied a SVM to identify the arc fault. Liu et al. [24] extracted the Hurst exponent, harmonic variance, and wavelet energy entropy of the current signal as the fault features, and combined CNN with LSTM to detect the arc fault. Du et al. [25] selected the time-domain, frequency-domain, and time-frequency domain features of the current signal by using the proposed two feature selection methods, and applied a K-nearest neighbor algorithm to detect the arc fault. Ren et al. [26] utilized a phase space reconstruction method to extract the chaotic features from the current and voltage signals, and used a LSTM to identify the arc fault.

Scholars at home and abroad have obtained a lot of research results in the field of arc fault. They have played an important role in promoting the development of arc fault circuit breakers. However, there are still the following issues.

1) The feature extraction and identification methods proposed in [2], [3], [4], [5], [6], [7], [8], [9], [10], [11], [12], [13], [14], [15], [16], [17], [18], [19], [20], [21], and [22] are mainly aimed at the series arc fault. Due to the current of the parallel arc fault is small, the weak raw fault features are easily submerged by the normal working current of the load. Therefore, the existing methods are difficult to detect the parallel arc fault.
2) In [23], [24], [25], and [26], the research on the feature extraction and identification method of the parallel arc fault is mainly aimed at the civilian and aviation fields. In the industrial three-phase power supply and distribution systems, both the power supply and typical loads are quite different from that in the civilian and aviation systems. Therefore, the above methods are difficult to directly apply to the industrial field.

Due to the fault current will be superimposed on the normal working current of the load, the weak parallel arc fault features are easily submerged by the normal working current. In addition, the current signal has obvious broadband features when the arc fault occurs in the circuit. The frequency band of the signal can be generally from several Hz to tens of MHz, and the high-frequency components will increase significantly [1], [2], [4], [8], [12], [13]. However, the amplitudes of the high-frequency components are relatively small. Due to the strong randomness and instability of the arc fault [4], [5], [10], [15], [19], the frequency band of the fault features in the arc fault current signal is complex and changeable. So, it is difficult to determine the fault features of the waveforms in various load circuits in the distribution network by using a fixed division frequency band [15]. Therefore, it is necessary to study the feature enhancement and extraction method of the parallel arc fault to realize the detection of the parallel arc fault.

In order to solve the abovementioned problems, the signal decomposition methods such as EWT [15], [16], VMD [17], CEEMD [18], and CEEMDAN [19], [20] have been widely applied to the field of arc fault detection, and have obtained a good performance on the feature extraction. However, for most of these methods, the signal decomposition algorithms were first performed on the current signals, and then the features of each modal component were extracted separately to obtain the arc fault features. As a result, there was a lack of correlation among the modal components in the extracted arc fault features.

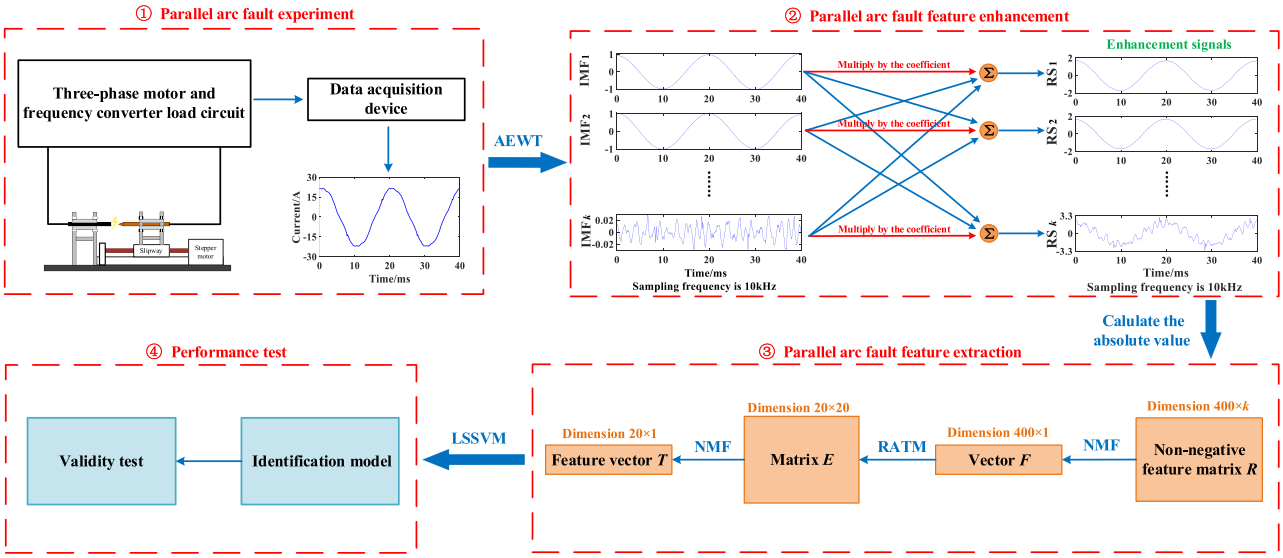

Fig. 1. Flowchart of the proposed idea.

It will affect the detection performance of the arc fault detection method. In response to the above issues, the parallel arc fault experiments were carried out in the typical industrial load circuit, and a new idea of the fault feature enhancement and extraction was proposed in the article. It uses the complete frequency band features of the parallel arc fault in the current signal to realize the parallel arc fault detection. Since, the amplitudes of the high-frequency features of the arc fault current signals are very small, they are very easy to be lost in the feature extraction process. In order to solve this problem, an arc fault feature enhancement method was proposed in this article. The current signal was decomposed into multiple modal components in different frequency bands by using the signal decomposition method, and the high-frequency components with smaller amplitude were amplified, then the feature enhancement signals were obtained by reconstructing these signals. On the basis of retaining the complete frequency band features of the arc fault, this method can amplify the rich high-frequency components of the arc fault features in the current signal, and enhance the weak parallel arc fault features in the original current signal by increasing the energy ratio of the arc fault feature signals in the current signal. In this way, it converts the current signal with weak parallel arc fault features into the feature enhancement signals with strong fault features. It makes the subsequent feature extraction method be able to effectively extract the features of the parallel arc fault. In order to obtain low-dimensional fault features from a matrix composed of multiple feature enhancement signals to detect the parallel arc fault, it is necessary to use non-negative matrix factorization (NMF) to reduce the dimension of the feature enhancement signals and retain the main features. The NMF is a common data dimension reduction method, it can decompose the original matrix into a product of a base matrix and a coefficient matrix by adding nonnegativity constraints. Due to nonnegativity constraints, on the one hand, there is no subtraction operation in the whole decomposition process, and there are only addition operations between the data, so the features will not offset each other. On the other hand, the decomposed results are the low-dimensional approximation of the original data and represent the essential features of the original data [27]. Therefore, the low-dimensional data obtained from the feature enhancement signals by using NMF can still approximately retain the features of the parallel arc fault in the feature enhancement signals. It can realize the feature extraction of the parallel arc fault. The flowchart of the proposed idea is shown in Fig. 1. The whole idea is composed of four parts: parallel arc fault experiment, parallel arc fault feature extraction, parallel arc fault feature enhancement and performance test. The specific is as follows. First, the current signal was obtained by conducting the parallel arc fault experiments. The adaptive empirical wavelet transform (AEWT) was used to adaptively decompose the current signal into k modal components, and k feature enhancement signals were obtained by multiplying the single modal component by an energy coefficient in turn and then reconstructing these signals. Third, a two-stage NMF dimension reduction method was proposed. k enhancement signals were first reduced into a 1-D signal by using the NMF, so that the influence of the number of decomposition layers on the number of the features can be eliminated. And an RATM was constructed by using the 1-D signal. To realize the extraction of the fault features, the RATM was reduced into a 1-D feature vector by reusing the NMF. Finally, the performance of the proposed method was tested by using the identification model established with a least squares support vector machine (LSSVM).

The main innovations and academic contributions of the article are as follows.

1) The experiments and the detection method of the parallel arc fault in the three-phase motor and frequency converter load circuit were studied for the first time. It can further broaden the research scope of the arc fault and provide reference for the development of industrial arc fault circuit breakers with parallel arc fault detection function, so as to effectively prevent electrical fires and other safety accidents caused by the parallel arc fault.

2) A new method of the parallel arc fault feature enhancement based on the energy transformation and reconstruction of each modal component decomposed by AEWT was proposed. This method can enhance the high-frequency fault features in the arc fault current on the basis of retaining the complete frequency band features. It can solve to some extent the problem of lacking the correlation among the decomposed signals, which usually appears when the fault features are extracted directly from the decomposed components. It can provide a new idea for the enhancement of weak fault features such as the arc fault features.
3) The NMF was applied to the field of the arc fault feature extraction for the first time, and a new method of the fault feature extraction based on two-stage NMF dimension reduction and RATM was proposed. The number of fault features extracted by this method can avoid the influence of the number of signal decomposition layers. It can provide reference for the fault feature extraction of the signal decomposition method with adaptive decomposition layers.

The rest of this article is organized to the four parts of Fig. 1. They are as follows. Section II describes the experimental platform and experimental scheme of the parallel arc fault, and briefly analyzes the current signal. Section III introduces the basic theory of AEWT in detail, and provides an arc fault feature enhancement method using decomposed signals multiplied by the energy coefficient and reconstruction. Section IV introduces the theory of the fault feature extraction method based on two-stage NMF dimension reduction and RATM. Section V establishes a parallel arc fault identification model, and presents the test results of the proposed methods. Finally, Section VI concludes this article.

II. Parallel Arc Fault Experiment

A. Experimental Platform and Experimental Scheme

The parallel arc fault experimental platform built by two typical industrial loads of the three-phase motor and frequency converter is shown in Fig. 2. The platform is mainly composed of the main circuit, arc fault generator and data acquisition device.

A three-phase power supply was used as the experimental power supply of the main circuit. Its rated output voltage is ac 380 V, and its rated output frequency is 50 Hz. A VFD110E43A type frequency converter and a Y160M-6-11 kW type three-phase asynchronous motor were used as the experimental loads. The loads were switched by contactor 1 and contactor 2, and the current of the three-phase motor load was adjusted by a friction load.

A flat carbon rod and a pointed copper rod of the arc fault generator were, respectively, used as the stationary and movable electrodes. The horizontal movement of the movable electrode was realized by controlling a stepping motor. The stationary and movable electrodes were connected in series with a current-limiting resistor and then connected in parallel in the A-phase and B-phase lines of the main circuit. The normal working state of the circuit was simulated by the separation of the stationary and movable electrodes. The arc fault state was simulated by controlling the movable electrode. Under the well contact of the stationary and movable electrodes condition, making the two

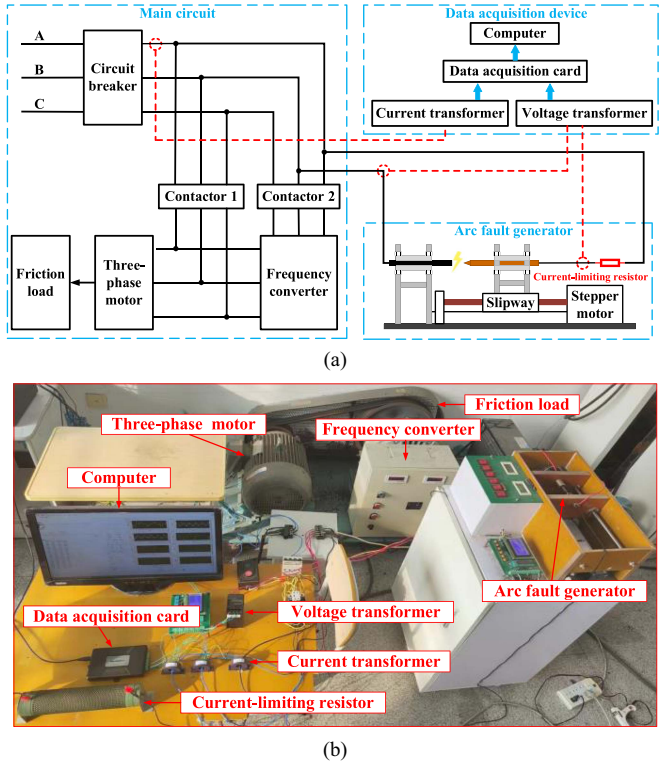

Fig. 2. Experimental platform. (a) Structure. (b) Photo.

TABLE I
Experimental Scheme

Group *No.*	Load type	Current-limiting resistor *R* /Ω	Load current *I* /A	Working condition
1-6	Three-phase motor	400	15, 18, 20	Normal, Fault
7-12	Three-phase motor	200	15, 18, 20	Normal, Fault
13-18	Three-phase motor	130	15, 18, 20	Normal, Fault
19-24	Frequency converter	400	15, 18, 20	Normal, Fault
25-30	Frequency converter	200	15, 18, 20	Normal, Fault
31-36	Frequency converter	130	15, 18, 20	Normal, Fault

The data acquisition device adopted a LHB100A5VY2 type current transformer and a LHB-T1 type voltage transformer to collect the A-phase line current and the arc voltage, respectively. The data were uploaded to a computer by using a USB3200 type data acquisition card, and then they were displayed and stored by using a Labview software.

The experiments were conducted under the normal and parallel arc fault states by utilizing the experimental platform shown in Fig. 2. The experimental scheme is shown in Table I. The experiments under the three-phase motor load condition were conducted by connecting contactor 1 and breaking contactor 2, while the experiments under the frequency converter load condition were conducted by breaking contactor 1 and connecting contactor 2. The current-limiting resistor of the parallel arc fault was 130 Ω, 200 Ω, and 400 Ω, respectively. The load current was set to 15 A, 18 A, and 20 A by adjusting the friction load. The carrier frequency and operating frequency of the frequency converter were set to 8 kHz and 50 Hz, respectively, and the data

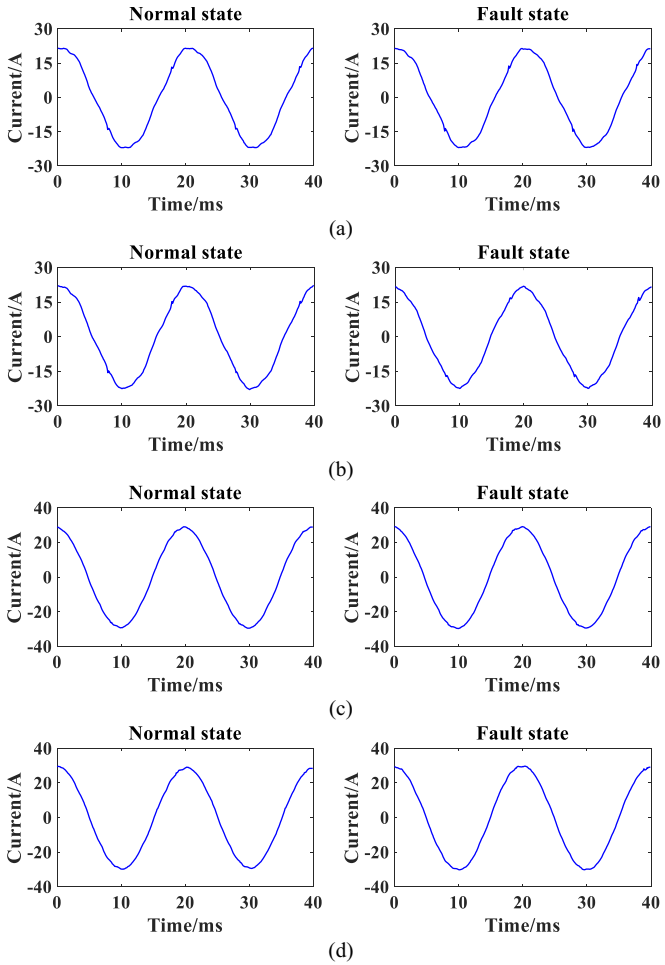

Fig. 3. Current waveforms of the three-phase motor load circuit. (a) I = 15 A, R = 400 Ω. (b) I = 15 A, R = 130 Ω. (c) I = 20 A, R = 400 Ω. (d) I = 20 A, R = 130 Ω.

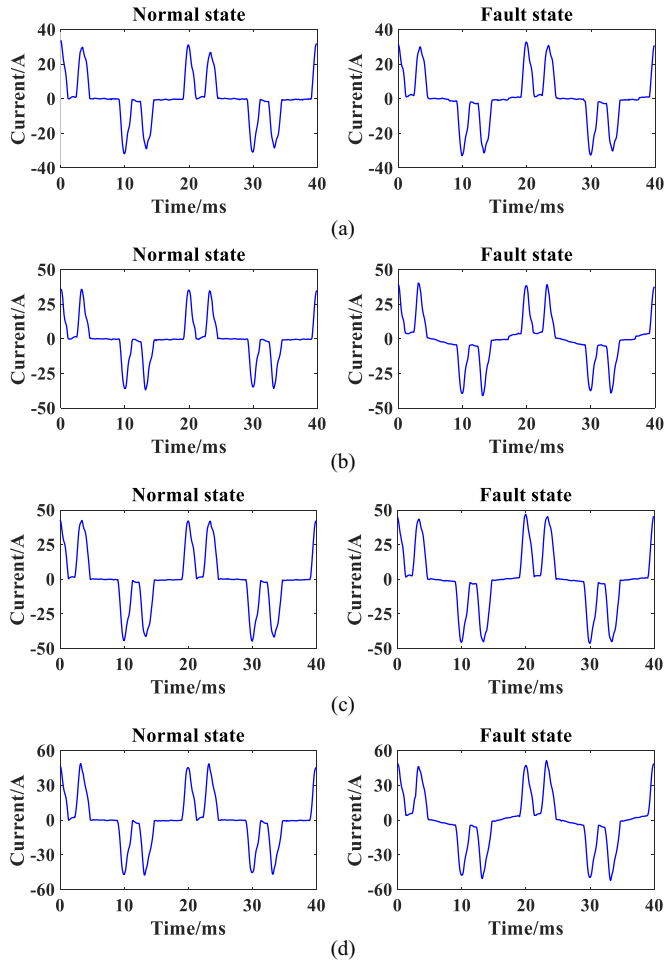

Fig. 4. Current waveforms of the frequency converter load circuit. (a) I = 15 A, R = 400 Ω. (b) I = 15 A, R = 130 Ω. (c) I = 20 A, R = 400 Ω. (d) I = 20 A, R = 130 Ω.

B. Analysis of Experimental Results

The current waveforms of the three-phase motor load circuit are shown in Fig. 3. The normal load current of the three-phase motor is an approximate sinusoidal signal. In the fault state, the circuit current waveform is the sum of the normal load current and the parallel fault branch current. The current signal on the parallel fault branch is the arc fault current signal of the resistive load. Although there are some phenomena such as zero-current and the increase of the high-frequency components in the arc fault current signal, the current waveform basically changes according to the sine law, and the normal load current amplitude is relatively large. Therefore, the features will be submerged by the superposition of the fault branch current signal and the normal load current signal. Under the same experimental conditions, it is difficult to find the difference of the current waveforms between the normal state and the fault state.

The current waveforms of the frequency converter load circuit are shown in Fig. 4. The frequency converter is a nonlinear load. In the normal state, the load current presents double-peak characteristics and exhibits a prolonged flat shoulder phenomenon. When the parallel arc fault occurs, an arc fault current signal with approximate sinusoidal law will be superimposed on the normal load current signal, so as to cause a certain upward and downward trend in the flat shoulder position. By comparing the circuit current waveforms under different load current and current-limiting resistor conditions, it can be seen that as the working current of the frequency converter and current-limiting resistor increases, the features in the flat shoulder position will be weakened. When the load current is 20 A and the current-limiting resistor is 400 Ω, it is also difficult to find the difference of the current waveforms between the normal state and the fault state.

III. Fault Feature Enhancement Method Based on AEWT and the Energy Transformation and Reconstruction of Modal Components

A. Basic Theory of AEWT

The EWT is a signal decomposition method that combines the adaptive decomposition concept of empirical mode decomposition (EMD) method and the tightly supported framework of wavelet transform theory. The method can overcome the modal mixing problem caused by the discontinuous time-frequency scale of the signal. It also has a complete and reliable

mathematical theory basis and low computational complexity. And the problem of overenvelope and underenvelope in EMD method can be solved by using EWT.

The EWT can adaptively divide the Fourier spectrum according to the signal features, and extract the modal components with a set of orthogonal wavelet filters. The detailed principle can refer to [15] and [16]. When using EWT decomposition, the number of decomposition layers of the signal should be set first. For the current signals under different loads and experimental conditions, the corresponding optimal EWT decomposition level is not a fixed value. The use of fixed decomposition level will make it lack the adaptability to the current signal, so as to affect the arc fault feature extraction and identification.

The EMD is an adaptive time series decomposition method based on Hilbert transform. It can adaptively decompose the signal based on the signal features without presetting the number of decomposition layers and frequency band, and objectively reflect the number of internal modes contained in the time series signal [28]. Therefore, the number of decomposition layers of EWT was determined based on EMD to realize the AEWT. However, if the number of decomposition layers determined by EMD is too small, the modal components obtained by AEWT will be less and the corresponding frequency band will be wider. During the process of the feature enhancement, it will result in poor enhancement effect of the signal in the fault feature frequency band with smaller energy in the modal components. In order to avoid the problem, the minimum number of decomposition layers of AEWT is limited to enhance the signals in multiple feature frequency bands. The specific method of the decomposition layers k is as follows.

The number of determining adoptively EMD modes n was obtained by utilizing EMD to decompose the current signal firstly. When n is less than or equal to 4, the number of EWT decomposition layers k is set to 4. When n is greater than 4, the number of EWT decomposition layers k is set to n. So the number of EWT decomposition layers k can be adaptively determined according to the above method.

B. Feature Enhancement Method Based on Energy Transformation and Reconstruction of Modal Components

To retain the complete frequency band features of the arc fault in the circuit current signal and enhance the weak parallel arc fault features, a feature enhancement method based on the energy transformation and reconstruction of modal components was proposed. The current signal was normalized by the effective value and decomposed into k modal components by using AEWT, and then each modal component was multiplied by an energy transformation coefficient and reconstructed to obtain k fault feature enhancement signals. The selection of the number of current signal cycles has an important influence on the detection performance of the parallel arc fault. The smaller the number of the current signal cycles selected in the analysis, the less the feature information of the parallel arc fault will be contained in the signal. It will lower the detection accuracy of the parallel arc fault. The increase of the number will enrich the feature information, but it will increase the calculation amount and operation time of the parallel arc fault detection method. By comprehensively considering the above two aspects, the number of current signal cycles used for analysis was finally set to 2, i.e., each current signal has 400 sampling points. The specific expressions are as follows:

$$\begin{cases} RS_1 = \gamma \times \eta_1 \times IMF_1 + IMF_2 + \cdots + IMF_k \\ RS_2 = IMF_1 + \gamma \times \eta_2 \times IMF_2 + \cdots + IMF_k \\ \qquad\qquad \vdots \\ RS_k = IMF_1 + IMF_2 + \cdots + \gamma \times \eta_k \times IMF_k \end{cases} \tag{1}$$

$$\eta_j = 1/\sqrt{\frac{1}{400}\sum_{i=1}^{400} IMF_j(i)^2} \tag{2}$$

where, $IMF_1, IMF_2, \ldots, IMF_k$are the modal components obtained by AEWT. $RS_1, RS_2, \ldots, RS_k$ are k fault feature enhancement signals. $\gamma$is the energy coefficient, it can be set according to the actual application scenario. And$j = 1, 2, \ldots, k$.

According to (1) and (2), the proposed fault feature enhancement method can make the reconstructed signals contain the parallel arc fault features in complete frequency band. And the parallel arc fault features in different frequency bands can be enhanced by performing an energy transformation on each modal component.

C. Performance of Feature Enhancement

The current signals in Figs. 3(c) and 4(c) were decomposed by utilizing AEWT, and the energy transformation and reconstruction of the modal components were performed by using the feature enhancement method proposed in Section III-B. The energy coefficient γ was set to 0.5. The feature enhancement signals are shown in Fig. 5.

The parallel arc fault features of the raw circuit current are quite weak. However, the feature enhancement signal RS_4 of the three-phase motor load and the feature enhancement signal RS_6 of the frequency converter load are obviously different in the normal state and fault state after the feature enhancement. It can provide favorable conditions for the subsequent parallel arc fault feature extraction.

IV. Fault Feature Extraction Method Based on NMF

A. Basic Theory

1) Non-Negative Matrix Factorization: NMF is a data dimension reduction method. It is widely used in pattern recognition, data mining, and information retrieval, but it has not been applied in the field of arc fault feature extraction. NMF can be divided into multiplicative update algorithm, gradient descent algorithm and alternating least squares algorithm. The multiplicative update algorithm was adopted in the article because of its low complexity and stable convergence.

A non-negative data matrix $A = [x_1, x_2, \ldots, x_N] \in R_+^{(m\times n)}$ is determined, and all elements of matrix A are non-negative. NMF aims to find two low-rank non-negative matrices W and H, to make the product of the two matrices will approximate the matrix A, i.e., $A_{(\mathrm{m}\times n)} \approx W_{(\mathrm{m}\times l)} \times H_{(l\times n)}$. Where,

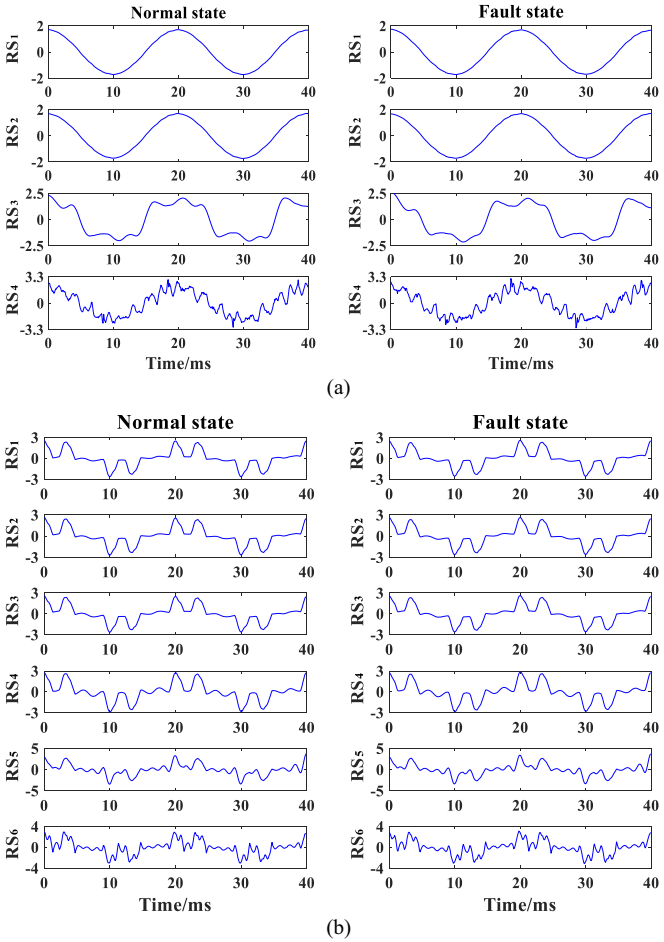

Fig. 5. Feature enhancement signals. (a) Three-phase motor load. (b) Frequency converter load.

$W = [w_m k] \in R_+^{(m\times l)}$, and $H = [h_l n] \in R_+^{(l\times n)}$, W and H are called the base matrix and the coefficient matrix, respectively, m, l, n are the dimension of data, the rank of factorization, and the size of data, respectively, $l \leq mn/(m+n)$. Then the base data matrix of l features is included in the matrix W, i.e., the target matrix after dimension reduction. The NMF based on Frobenius norm was adopted in the article. It can be expressed as follows:

$$O_F = \left\|\mathbf{A} - WH^T\right\|_F^2 \quad \text{s.t.} W \geq 0, H \geq 0 \tag{3}$$

where $\|\cdot\|_F$ is the Frobenius norm of the matrix.

The iterative multiplication updating algorithm of the objective function (3) is as follows:

$$w_{ml} \leftarrow w_{ml} \frac{(AH)_{ml}}{(WH^{\mathrm{T}}H)_{ml}} \tag{4}$$

$$h_{ln} \leftarrow h_{ln} \frac{(A^{\mathrm{T}}H)_{ln}}{(H^{\mathrm{T}}HW^{\mathrm{T}})_{ln}} \tag{5}$$

where $W = [w_{ml}]$,$H = [h_{ml}]$.

The initial matrices W_0 and H_0 can be randomly generated during the update calculation. When the termination condition of the iteration is given, it is updated alternately according to (4) and (5). When the iteration termination condition is satisfied, the target matrices W and H are obtained [29].

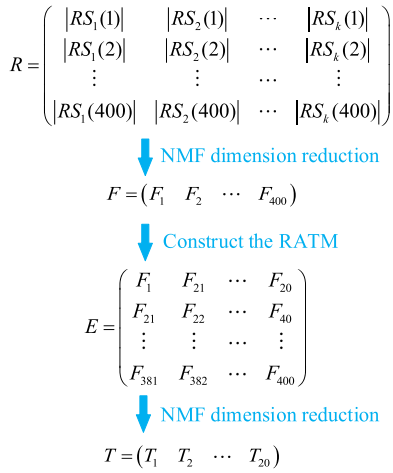

Fig. 6. Principle of fault feature extraction method.

2) Reconstructed Attractor Track Matrix: The attractors trajectories matrix (ATM) is a common method of architecting a matrix for time series signals. Assuming a 1-D discrete signal with length n is Y, where,$Y = [y_1, y_2, \ldots, y_n]$, then the corresponding ATM is constructed as follows:

$$A = \begin{bmatrix} y_1 & y_2 & \cdots & y_i \\ y_2 & y_3 & \cdots & y_{i+1} \\ \cdots & \cdots & \cdots & \cdots \\ y_m & y_{m+1} & \cdots & y_n \end{bmatrix} \tag{6}$$

where $1 < i < n$, $m = n - i + 1$.

Conventional ATM is also called Hankel matrix. The data of adjacent rows in the constructed matrix differ by only one data point. Therefore, the problems such as high data correlation between adjacent rows and high operation cost are caused. In view of the above problems, a time delay step t can be reasonably introduced. Then, an RATM is obtained, and its expression is as follows [16]:

$$A = \begin{bmatrix} y_1 & y_2 & \cdots & y_i \\ y_{1+t} & y_{2+t} & \cdots & y_{i+t} \\ \cdots & \cdots & \cdots & \cdots \\ y_{1+(m-1)t} & y_{2+(m-1)t} & \cdots & y_{i+(m-1)t} \end{bmatrix}. \tag{7}$$

B. Fault Feature Extraction Method Based on Two-Stage NMF Dimension Reduction and RATM

The principle of the fault feature extraction method based on two-stage NMF dimension reduction and RATM is shown in Figs. 1 and 6. The feature enhancement method proposed in Section III was used to deal with the current signal with 400 sampling points, and a $400 \times k$ dimensional non-negative feature matrix R was constructed by utilizing the absolute values of the obtained k feature enhancement signals. Then, the non-negative feature matrix R was reduced to a vector F by using NMF. The delay step of RATM was set to 20, and a 20×20 dimensional matrix E was constructed by using the vector F. A

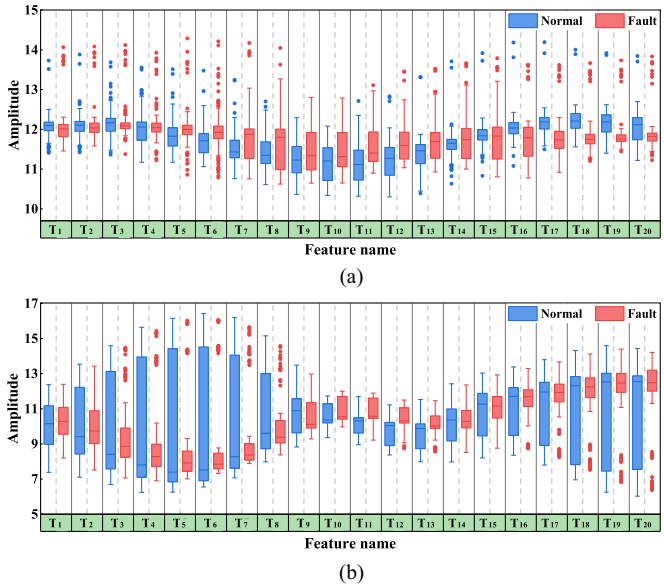

Fig. 7. Distribution of parallel arc fault features. (a) Three-phase motor load. (b) Frequency converter load.

1×20 dimensional vector T was obtained by reusing NMF to reduce the dimension of the matrix E, and the elements in the vector T were the features of the parallel arc fault.

C. Analysis of Parallel Arc Fault Features

When the load current is 20 A and the current-limiting resistor is 400 Ω, 100 current signals in the normal state and 100 current signals in the fault state were intercepted from the experimental data of the three-phase motor and frequency converter loads, respectively. The number of sampling points of each current signal is 400.

The parallel arc fault features were extracted by using the fault feature extraction method proposed in Section IV-B. The distribution of these fault features is shown in Fig. 7. There are obvious differences in the distribution range of some features between the normal state and the fault state, such as, the features T_{18} and T_{19} of the three-phase motor load, and the features T_{11} and T_{12} of the frequency converter load.

V. Performance Test of Parallel Arc Fault Features

A. Parallel Arc Fault Identification Model and Validity Test of Features

1) POA-LSSVM Identification Model: To verify the validity of the extracted parallel arc fault features, a parallel arc fault identification model was established with an LSSVM. LSSVM is a machine learning algorithm based on SVM. It is mainly applied in data regression, pattern classification and identification. The algorithm reduces the parameter search range from 3-D to 2-D by transforming the quadratic programming problem in SVM into the solution of linear equations. It can greatly ensure the calculation accuracy, reduce the computational complexity and improve the calculation speed. The performance of the LSSVM identification model is affected by the selection of penalty coefficient c and kernel parameter g [30]. In order to select the optimal parameters to improve the performance of the identification model, a pelican optimization algorithm (POA) was used to optimize the parameters c and g.

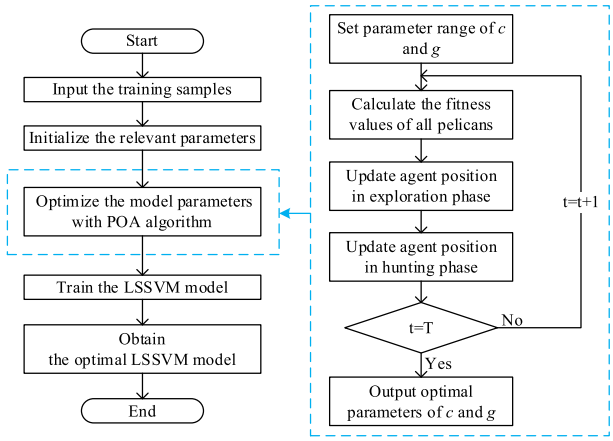

Fig. 8. Process of LSSVM optimized by POA.

POA is a new algorithm based on the natural behavior of pelicans. The algorithm can simulate the behavior and strategy of pelican population foraging, so as to transform the optimization problem into the process of parameter search. The optimal parameters can be found through the two-stage iteration of exploration and hunting, so that it has better global search ability and convergence speed [31]. The process of LSSVM optimized by POA is shown in Fig. 8.

2) Results of Validity Test of the Parallel Arc Fault Features: There are 36 groups of experiments in Table I. For each group of experiments, 500 segments of current signal were intercepted. The corresponding fault features were calculated by using the proposed feature enhancement and extraction method and constructed as a sample set. The category labels of the fault features extracted from the current signals in the normal state and fault state were set to 0 and 1, respectively. Then, the sample set was divided into the training samples and the test samples on average, and one twentieth of the training samples was selected and used as the optimization samples.

The population size of POA was set to 20, and the maximum number of iterations was set to 40. The optimal parameters c and g can be obtained by the optimization samples. They are 39.84 and 0.01, respectively. An LSSVM identification model was established with the training samples and the optimal parameters c and g. The tests were carried out by inputting the testing samples into the LSSVM identification model. The identification results of the parallel arc fault are shown in Figs. 9 and 10.

As seen in Figs. 9 and 10, the following three conclusions can be obtained.

1) Under different experimental conditions, the detection accuracy of the parallel arc fault is higher than 95%. Among them, the true positive rate is higher than 93.87%, and the false positive rate is lower than 3.47%. It was verified that the proposed method can accurately detect the parallel arc fault occurred in the three-phase motor and frequency converter load circuit.

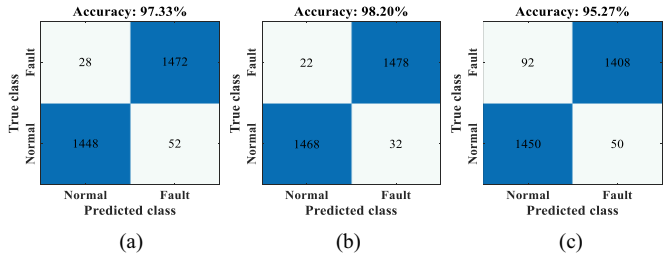

Fig. 9. Identification results of parallel arc fault in the three-phase motor load circuit. (a) R = 130 Ω. (b) R = 200 Ω. (a) R = 400 Ω.

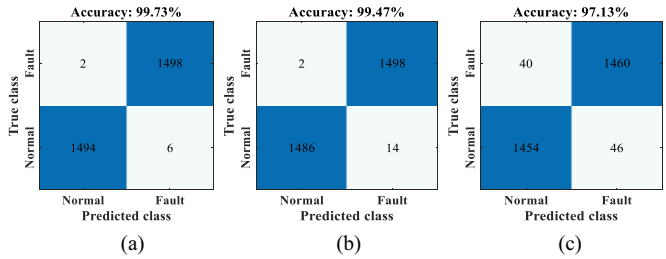

Fig. 10. Identification results of parallel arc fault in the frequency converter load circuit. (a) R = 130 Ω. (b) R = 200 Ω. (a) R = 400 Ω.

2) The detection accuracy of the parallel arc fault in the frequency converter load circuit is obviously higher than that in the three-phase motor load circuit. Due to the current signal of the parallel fault branch is an approximate sinusoidal signal, which is similar to the normal load current signal of the three-phase motor load circuit. So, the fault features are more difficult to extract from the current signal, leading to a lower detection accuracy.
3) Compared with 130 Ω and 200 Ω, when the current-limiting resistor is 400 Ω, the detection accuracy of the parallel arc fault is lower. When the current-limiting resistor is larger, the fault branch current will be smaller, so the fault features will be weaker.

To evaluate the real-time performance of the proposed method, the detection time for the parallel arc fault was systematically tested. The detection time is mainly composed of two parts. One is the time required to collect the current data. The current signal analyzed by the proposed method is two cycles, so it needs to take 40 ms to collect the current signal of two complete cycles. The other is the operation time of the algorithm, which is measured from the completion of the current signal acquisition to the detection result of the parallel arc fault is obtained. The average operation time of the algorithm under a computer test condition is 2.7 ms. The hardware platform and software environment of the computer tests are mainly as follows. The CPU of the computer is Intel (R) Core (TM) i5-9500 with 3 GHz main frequency, and the memory is 8 GB. The operating system of the computer is 64-bit Windows 10. The program codes of the proposed detection method are written and run in a MATLAB 2023b software, which is installed on the computer. Therefore, in the above hardware platform and software environment, a total of 42.7 ms is required for a single complete detection process. It is the time interval from initial signal acquisition to final diagnostic conclusion. It can meet the real-time requirements of IEC 62606 standard for the arc fault detection [32].

TABLE II
DETECTION ACCURACY OF DIFFERENT DECOMPOSITION METHODS WITH AND WITHOUT FEATURE ENHANCEMENT METHOD

Decomposition method	Feature enhancement method	Detection accuracy /%
EMD	Without	72.84
EMD	With	78.61
VMD	Without	88.11
VMD	With	91.99
EWT	Without	82.96
EWT	With	97.85

B. Validity Verification of the Feature Enhancement Method

In order to verify the validity of the proposed feature enhancement method, the detection accuracy of the parallel arc fault was tested and compared by using different decomposition methods with and without the feature enhancement method. Three decomposition methods were used. They are EMD, VMD, and EWT, respectively. The test results are shown in Table II. When using VMD and EWT, the number of decomposition layers was determined according to the adaptive decomposition layer determination method proposed in Section III-A. Without feature enhancement method means that there is no energy transformation and reconstruction of the modal components. For all the methods in Table II, the same feature extraction method, identification model and test method were used.

As seen in Table II, for each signal decomposition method, the detection accuracy of the parallel arc fault will be obviously improved when the proposed feature enhancement method was used. It can verify the validity and versatility of the feature enhancement method. Besides, it can be seen that the performance of EWT is better than that of EMD and VMD under the conditions of using the feature enhancement method.

C. Comparison With Existing Arc Fault Feature Extraction Methods

In order to verify the superiority of the proposed feature extraction method, nine similar feature extraction methods were selected from the existing research methods, and used to test and compare the detection performance. Among them, the methods proposed in [4], [7], [12], [15], and [21] are mainly applied to the series arc fault in the single-phase ac load circuit in the civilian field, and the methods proposed in [16] and [17] are mainly applied to the series arc fault in the three-phase motor and frequency converter load circuit in the industrial field. And the methods proposed in [23] and [24] are mainly applied to the parallel arc fault in the aviation field.

The feature extraction processes of the abovementioned methods are as follows.

1) *In* [4]*:* The average value of the absolute values, the sum of the harmonic amplitudes and the wavelet energy entropy of the current signal were extracted and used as the fault features.

2) *In* [7]*:* The current signal was reconstructed by using phase space transformation. From phase space, a similarity matrix was constructed by using the Euclidean distance. Then, the original signal was transformed into a gray-scale image. Finally, the textural image features were extracted from the image by using the gray-level co-occurrence matrix and used as the fault features.
3) *In* [12]*:* The high-frequency reconstructed signals of the current signal were constructed by using wavelet reconstruction theory, and the integral, variance, kurtosis, and Shannon entropy of the high-frequency reconstructed signals were extracted and used as the fault features.
4) *In* [15]*:* The current signal was decomposed by using EWT. Then, the composite entropy of the fifth modal component such as the sample entropy, fuzzy entropy, permutation entropy, and approximate entropy were calculated, and the time-domain sensitive features of the current signal such as the variance, mean, kurtosis, margin factor, waveform factor, pulse factor, root mean square, skewness, and the average value of the absolute values were calculated. Finally, the composite entropy and the time-domain sensitive features were fused and used as the fault features.
5) *In* [16]*:* The five-layer EWT of the current signal was conducted, then the RATM of each layer of decomposed signal was constructed. And the first two singular values of the RATM were calculated and used as the fault features.
6) *In* [17]*:* The current signal was adaptively decomposed by using a VMD, and the energy entropy and sample entropy of the decomposed signals in the feature frequency band were extracted and used as the fault features.
7) *In* [21]*:* The kurtosis, crest factor, clearance factor, *L2/L1* norm, shape factor and spectral centroid of the current signal were extracted and used as the fault features.
8) *In* [23]*:* The signal component with the frequency of 2 kHz of the current signal was extracted by using the generalized S-transform, and the root mean square and energy of the component were calculated and used as the fault features.
9) *In* [24]*:* The time-domain Hurst exponent, harmonic variance, and wavelet energy entropy of the current signal were calculated and used as the fault features.

The detection accuracy of the parallel arc fault for the above-mentioned fault features were tested by utilizing the identification model and test method proposed in Section V-A, and the test results are shown in Table III.

The detection accuracy of the parallel arc fault of the proposed feature enhancement and extraction method is obviously higher than that of the other nine methods. It can verify the superiority of the proposed method in the parallel arc fault detection.

D. Validity Verification of the Method Under the Conditions of Speed Variation

In the industrial field, the three-phase motor often works under the conditions of acceleration, deceleration, and speed fluctuation. In most cases, the speed of the three-phase motor was adjusted by changing the operating frequency of the frequency converter. To verify the validity of the proposed method under the conditions of speed variation, the parallel arc fault experiments under the speed variation conditions were carried out by using the experimental platform in Fig. 2. The experimental scheme is shown in Table IV. Among them, the increase of the speed was realized by increasing the operating frequency of the frequency converter gradually from 30 to 50 Hz, the decrease of the speed was realized by reducing the operating frequency of the frequency converter gradually from 50 to 30 Hz. The fluctuation of the speed was realized by adjusting the operating frequency of the frequency converter between 35 and 45 Hz.

The proposed method was applied to detect the parallel arc fault for the experiments under the speed variation conditions, and the detection accuracy can reach 95.80%. It can verify that the validity of the proposed method under the speed variation conditions.

TABLE III
DETECTION ACCURACY OF THE PARALLEL ARC FAULT WITH DIFFERENT FEATURE EXTRACTION METHODS

Method *No.*	Feature extraction method	Detection accuracy /%
1	Reference [4]	87.66
2	Reference [7]	91.38
3	Reference [12]	70.51
4	Reference [15]	92.94
5	Reference [16]	90.88
6	Reference [17]	80.33
7	Reference [21]	92.49
8	Reference [23]	62.97
9	Reference [24]	70.70
10	Proposed method	97.85

TABLE IV
EXPERIMENTAL SCHEME UNDER SPEED VARIATION CONDITIONS

Group *No.*	Current-limiting resistor *R* /Ω	Speed variation condition	Working condition
1-6	400, 200, 130	Speed increase	Normal, Fault
7-12	400, 200, 130	Speed decrease	Normal, Fault
13-18	400, 200, 130	Speed fluctuation	Normal, Fault

TABLE V
EXPERIMENTAL SCHEME UNDER THE CONDITIONS OF DIFFERENT CARRIER FREQUENCIES OF THE FREQUENCY CONVERTER

Group *No.*	Current-limiting resistor *R* /Ω	Carrier frequency /kHz	Working condition
1-6	400, 200, 130	2	Normal, Fault
7-12	400, 200, 130	5	Normal, Fault
13-18	400, 200, 130	11	Normal, Fault
19-24	400, 200, 130	14	Normal, Fault

E. Validity Verification of the Method Under the Conditions of Different Carrier Frequencies of the Frequency Converter

The carrier frequency of the frequency converter often needs to be set according to the conditions of the industrial field. To verify the validity of the proposed method for the parallel arc fault detection under the conditions of different carrier frequencies, the parallel arc fault experiments under four conditions of the different carrier frequencies were carried out by using the experimental platform in Fig. 2. The experimental scheme is shown in Table V.

The proposed method was applied to detect the parallel arc fault for the experiments under the conditions of different carrier frequencies of the frequency converter, the detection accuracy can reach 99.85%. It can verify that the validity of the proposed method under the conditions of different carrier frequencies of the frequency converter.

VI. Conclusion

Aiming at the problem that there is no effective detection method for the parallel arc fault in the industrial field, a feature enhancement method based on energy transformation and reconstruction of the current decomposition signals, and a fault feature extraction method based on two-stage NMF dimension reduction and RATM were proposed. The main conclusions are as follows.

1) When a parallel arc fault occurs in the circuit, the fault features are very weak due to the influence of the normal working current of the load. And the parallel arc fault in the three-phase motor load circuit is more difficult to detect than those in the frequency converter load circuit under the same experimental conditions. So, it is necessary to use an appropriate fault feature enhancement method to solve the problem of the fault features submerged in the normal circuit current.
2) A feature enhancement method based on AEWT and the energy transformation and reconstruction of modal components was proposed. It can obviously enhance the parallel arc fault features of the current signal, and provide an effective means to simplify the fault feature extraction and improve the detection accuracy of the weak arc fault.
3) A fault feature extraction method based on two-stage NMF dimension reduction combined with RATM was proposed. It can effectively extract the fault features from the feature enhancement signals, and the number of features is independent of the number of signal decomposition layers. Combined with an LSSVM identification model, the detection accuracy of the parallel arc fault with the current-limiting resistor lower than 400 Ω in the three-phase motor and frequency converter circuit is higher than 95%. It can provide reference for the development of industrial arc fault circuit breakers.

The development of the parallel arc fault detection and protection device has not been carried out in this article, but the proposed detection algorithm of the parallel arc fault based on AEWT, NMF, and LSSVM can be implemented on the hardware platform of Raspberry Pi. Although Raspberry Pi is more expensive than DSP and other microprocessors, and it will increase the cost of the detection and protection device. In view of the fact that the parallel arc fault is an important risk factor for the equipment damage, electrical fire and other safety accidents, it is still necessary to develop the detection and protection device based on Raspberry Pi. Therefore, the next work will focus on the development of the detection and protection device by deploying the proposed method to a Raspberry Pi. It will provide an effective protection method for preventing electrical fires and other safety accidents caused by the parallel arc fault.

References

[1] G. Liu et al., "Research on LV arc fault protection and its development trends," *Power Syst. Tech.*, vol. 47, no. 5, pp. 305–313, Jan. 2017.

[2] Y. J. Wu, W. H. Choi, C. S. Lam, M.-C. Wong, S.-W. Sin, and R. P. Martins, "An FPGA-based self-reconfigurable arc fault detection system for smart meters," *IEEE Trans. Circuits Syst. II, Exp. Briefs*, vol. 69, no. 10, pp. 4133–4137, Oct. 2022.

[3] R. Jiang and Y. Zheng, "Series arc fault detection using regular signals and time-series reconstruction," *IEEE Trans. Ind. Electron.*, vol. 70, no. 2, pp. 2026–2036, Feb. 2023.

[4] Z. He et al., "The detection of series AC arc fault in low-voltage distribution system," *Trans. China Electrotechnical Soc.*, vol. 38, no. 10, pp. 2806–2817, May 2023.

[5] R. Ding et al., "Series arc fault detection in low-voltage AC power lines based on absolute difference of the neighboring waveform of the current and randomness," *Power Syst. Protection Control*, vol. 51, no. 8, pp. 169–178, Apr. 2023.

[6] X. Chen, J. Leng, and H. Li, "Series fault arc recognition method based on an all-phase spectrum and deep learning," *Power Syst. Protection Control*, vol. 48, no. 17, pp. 1–8, Sep. 2020.

[7] F. Ferracuti, P. Schweitzer, and A. Monteriù, "Arc fault detection and appliances classification in AC home electrical networks using recurrence quantification plots and image analysis," *Electric Power Syst. Res.*, vol. 201, Dec. 2021, Art. no. 107503.

[8] Y. Wang, L. Hou, K. C. Paul, Y. Ban, C. Chen, and T. Zhao, "ArcNet: Series AC arc fault detection based on raw current and convolutional neural network," *IEEE Trans. Ind. Inform.*, vol. 18, no. 1, pp. 77–86, Jan. 2022.

[9] T. Zhang, R. Zhang, H. Wang, R. Tu, and K. Yang, "Series AC arc fault diagnosis based on data enhancement and adaptive asymmetric convolutional neural network," *IEEE Sensors J.*, vol. 21, no. 18, pp. 20665–20673, Sep. 2021.

[10] S. Zhang, N. Qu, T. Zheng, and C. Hu, "Series arc fault detection based on wavelet compression reconstruction data enhancement and deep residual network," *IEEE Trans. Instrum. Meas.*, vol. 71, 2022, Art. no. 3508409.

[11] P. Zhang et al., "Research on time-frequency analysis and identification of series arc fault based on generalized S-transform," *Power Syst. Tech.*, vol. 48, no. 7, pp. 2995–3003, Jan. 2024.

[12] C. Luo et al., "Low voltage arc fault identification method based on high frequency reconstructed signal and bayes-XGBoost," *Power Syst. Protection Control*, vol. 51, no. 13, pp. 91–101, Jul. 2023.

[13] G. Long et al., "Series arc fault detection technology based on multi-feature fusion neural network," *High Voltage Eng.*, vol. 47, no. 2, pp. 463–471, Feb. 2021.

[14] Y. Zhang et al., "Lightweight AC arc fault detection method by integration of event-based load classification," *IEEE Trans. Ind. Electron.*, vol. 71, no. 4, pp. 4130–4140, Apr. 2024.

[15] Y. Wang et al., "Arc fault detection based on empirical wavelet transform composite entropy and feature fusion," *Power Syst. Tech.*, vol. 47, no. 5, pp. 1912–1919, May 2023.

[16] H. Gao, Z. Wang, C. Han, A. Tang, F. Guo, and B. Li, "Feature extraction method of series arc fault occurred in three-phase motor with inverter circuit," *IEEE Trans. Power Electron.*, vol. 37, no. 9, pp. 11164–11173, Sep. 2022.

[17] Z. Wang, C. Han, H. Gao, and F. Guo, "Identification of series arc fault occurred in the three-phase motor with frequency converter load circuit via VMD and entropy-based features," *IEEE Sensors J.*, vol. 22, no. 24, pp. 24320–24332, Dec. 2022.

[18] Y. Jiang et al., "Identification method of low voltage series fault arc based on improved CEEMD decomposition and RF," *Power Syst. Protection Control*, vol. 52, no. 1, pp. 97–108, Jan. 2024.

[19] Z. Zhang, J. Ren, X. Tang, S. Jing, and W.-J. Lee, "Novel approach for arc fault identification with transient and steady state based time-frequency analysis," *IEEE Trans. Ind. Appl.*, vol. 58, no. 4, pp. 4359–4369, Jul. 2022.

[20] G. Zou, G. Fu, B. Han, W. Wang, and C. Liu, "Series arc fault detection based on dual filtering feature selection and improved hierarchical clustering sensitive component selection," *IEEE Sensors J.*, vol. 23, no. 6, pp. 6050–6060, Mar. 2023.

[21] W. Dai, X. Zhou, Z. Sun, Q. Miao, and G. Zhai, "Series AC arc fault detection method based on *L*2/*L*1 norm and classification algorithm," *IEEE Sensors J.*, vol. 24, no. 10, pp. 16661–16672, May 2024.

[22] S. Hwang, B. Kim, M. Kim, and H.-P. Park, "AC series arc fault detection for wind power systems based on phase lock loop with time and frequency domain analyses," *IEEE Trans. Power Electron.*, vol. 39, no. 10, pp. 12446–12455, Oct. 2024.

[23] R. Cui, D. Tong, and Z. Li, "Aviation arc fault detection based on generalized S transform," *Proc. CSEE*, vol. 41, no. 23, pp. 8241–8250, Dec. 2021.
[24] X. Liu, D. Huang, T. Jing, and Y. Zhang, "Detection of AC arc faults of aviation cables based on H-I-W three-dimensional features and CNN-LSTM neural network," *IEEE Access*, vol. 10, pp. 106958–106971, 2022.
[25] L. Du, Z. Xu, H. Chen, and D. Chen, "Feature selection-based low-voltage AC arc fault diagnosis method," *IEEE Trans. Instrum. Meas.*, vol. 72, Oct. 2023, Art. no. 3534112.
[26] J. Ren, Z. Zhang, X. Tang, S. Jing, K. Liao, and W.-J. Lee, "Dynamic impedance and chaotic behavior modeling featured novel robust arc fault identification approach," *IEEE Trans. Ind. Appl.*, vol. 60, no. 2, pp. 2480–2490, Mar./Apr. 2024.
[27] D. D. Lee and H. S. Seung, "Learning the parts of objects by non-negative matrix factorization," *Nature*, vol. 401, no. 6755, pp. 788–791, Nov. 1999.
[28] P. Zhang et al., "Dissolved gas prediction in transformer oil based on empirical wavelet transform and gradient boosting radial basis," *Power Syst. Tech.*, vol. 45, no. 9, pp. 3745–3754, Sep. 2021.
[29] K. Qu, Z. Li, C. Wang, F. Luo, and W. Bao, "Hyperspectral unmixing using higher-order graph regularized NMF with adaptive feature selection," *IEEE Trans. Geosci. Remote Sens.*, vol. 61, 2023, Art. no. 5511815.
[30] Q. Ge et al., "Industrial power load forecasting method based on reinforcement learning and PSO-LSSVM," *IEEE Trans. Cybern.*, vol. 52, no. 2, pp. 1112–1124, Feb. 2022.
[31] S. Jamal, J. Pasupuleti, N. A. Rahma, and N. M. L. Tan, "Multi-objective optimal energy management of nanogrid using improved pelican optimization algorithm," *IEEE Access*, vol. 12, pp. 41954–41966, Mar. 2024.
[32] I. E. Commission et al. "General requirements for arc fault detection devices; IEC 62606," International Electrotechnical Commission: Geneva, Switzerland, 2017.

Hongxin Gao (Member, IEEE) received the B.S., M.S., and Ph.D. degrees in electrical engineering from Liaoning Technical University, Huludao, China, in 2013, 2015, and 2019, respectively.

He is currently an Associate Professor with Liaoning Technical University. His current research interests include electrical contact, electric arc, and intelligent electrical apparatus.

Yuze Lv received the B.S. degree in electrical engineering in 2023 from Liaoning Technical University, Huludao, China, where he is currently working toward the M.S. degree in electrical engineering.

His current research interests include electrical contact and electric arc.

Zhiyong Wang (Member, IEEE) received the B.S. and M.S. degrees in electrical engineering and the Ph.D. degree in safety management engineering from Liaoning Technical University, Huludao, China, in 2005, 2008, and 2017, respectively.

He is currently an Associate Professor with Liaoning Technical University. His current research interests include electrical contact, electric arc, and intelligent electrical apparatus.

Jiacheng Cai received the B.S. degree in electrical engineering from Liaoning Technical University, Huludao, China, in 2013, and the M.S. degree in control engineering from Northeast Electric Power University, Jilin, China, in 2016. He is currently working toward the Ph.D. degree in electrical engineering with Liaoning Technical University.

He is currently a Lecturer with Liaoning Technical University. His current research interests include electrical contact and electric arc.